ANALYSIS OF TRANSPORT PHENOMENA IN SUBMERGED ARC FURNACE FOR FERROCHROME PRODUCTION

Y. Yang, Y. Xiao and M.A. Reuter

Delft University of Technology, Dept. of Applied Earth Sciences
Mijnbouwstraat 120, 2628 RX Delft, The Netherlands. E-mail: y.yang@ta.tudelft.nl

ABSTRACT

Ferrochrome is the major chromium source for stainless steel production, and submerged-arc furnaces (SAF) are most commonly utilised to smelt chromite ores into ferrochrome by using suitable carbonaceous reductants such as coke. Because of the complexity of feed structure and electrical-thermal-chemical interactions, there exist large gradients and wide distributions of temperature, mineralogy and other process variables in the furnace. This leads to various zones in the furnace, and different reduction mechanisms. Control of the furnace is thus often difficult due to the complicated physical and chemical situations in the furnace. The temperature profile in the submerged arc furnace has a great influence on the reduction rate and the production efficiency. Therefore, the energy generation through electrical arcs submerged in the solid feed and its distribution within the packed bed play an important role. In the present paper, an overall process model is illustrated to simulate inter-linked transport processes of fluid flow, heat transfer and reduction kinetics within the submerged arc furnace. The application of reaction kinetic data to simulate the chromite pellet/lumpy ore reduction with CO gas is presented and further adjusted to provide a submodel for a flow and heat transfer simulation for the packed bed by using computational fluid dynamics (CFD) technique. The comprehensive process model is aimed to simulate materials and gas flow, temperature and energy distribution throughout the furnace system. A preliminary model for gas flow and temperature distribution for the upper part of a 20 MW furnace (the packed bed) for high carbon ferrochrome production has been developed under simplified conditions. The integration of the reaction kinetic model into process simulation, and the future vision for a more comprehensive process modelling are discussed. It is expected that better understanding of the furnace insights through process modelling will help process optimisation and furnace control.

1. INTRODUCTION

Rapid growth of the world stainless steel industry during the past two decades posts a high demand on the production of ferrochrome which is the main raw material for stainless steel production. Submerged-arc furnaces (SAF) are used to smelt chromite ores into ferrochrome by using a carbonaceous reductant (anthracite, char, coke). The energy consumption is relatively high, and for high carbon ferrochrome the electrical energy consumption varies between 2000 kWh/t alloy with pre-reduction to 4000 kWh/t alloy without pre-reduction and feed preheating. Because of the complexity of feed structure and electrical-thermal-chemical interactions, large temperature gradients exist in the furnace from a few hundreds at the surface of the burden to well over 2000°C around the electrode tips. This leads to various zones in the furnace and different reduction mechanisms, as is clearly exemplified by the dig-out of large scale industrial submerged arc furnaces for ferrochromium and ferromanganese furnaces [1-2]. In the furnace, a single chromite pellet or lumpy ore experiences an increasing temperature environment while the charge is descending, and is reduced by the ascending CO gas and promoted by contacted coke particles. It is obvious that temperature profile in the submerged arc furnace has a great influence on the reduction rate and the production efficiency. Due to the sensitivity of the electrode control system to the distribution of the furnace temperature, the temperature distribution within the feed and various reaction zones are usually not symmetrically distributed. This uneven temperature distribution causes the difficulties in furnace control, product quality, and furnace efficiency.

Proceedings: Tenth International Ferroalloys Congress; 1 – 4 February 2004
INFACON X: '*Transformation through Technology*' Cape Town, South Africa
ISBN: 0-9584663-5-1 Produced by: Document Transformation Technologies

In practice, it is very difficult to diagnose the internal status of the furnace, e.g. the temperature and velocity and pressure distribution at different levels and different radial locations. In order to control the furnace better, understanding the transport process within the furnace is essential and that could be gained through various types of simulation tools, and the link of process modelling and simulation to better process control has been elucidated by the authors [3]. Several attempts of using mathematical models to simulate the physical and chemical transport process within the submerged arc furnace have been made by various researchers [4-8]. Use of computational fluid dynamics (CFD) technique provides the possibility and convenience to simulate and link various transport phenomena which are normally expressed with second order partial differential equations. However, the overall process model based on CFD requires individual sub-models to provide detailed information for the pressure drop through the packed bed (flow in porous media), Lorentz body force to the gases and to the molten slag and alloy, Joule/arc heating and reduction energy consumption for heat transfer, reduction kinetic model for reduction degree and mass and energy source for flow and heat transfer models. For electric arc furnace (EAF) steelmaking a lot of research work has been carried out since 1980s [9-10]. Nevertheless, the EAF steelmaking involves only open arcs and the arcs interact with molten slag and steel only. Simulation of an electrical furnace with immersed electrode in molten melts has also been found in the literature for nonferrous smelting or slag cleaning operations [11-12]. The transport phenomena in such cases involve only the Joule heating and electromagnetic stirring for the melt flow. Simulation of the transport phenomena in electric smelting of nickel matte in a submerged arc furnace has also been reported [13-14], but the focus was on the slag matte interactions, and the solid feed was treated with boundary conditions.

Because of the extreme complexity of the submerged arc furnace, only a few studies were published for the simulation of submerged arc furnaces by using CFD technique [4-8]. Sridhar and Lahiri [4] reported a steady state model for current and temperature distributions in a submerged arc furnace for ferromanganese production. A 2-dimensional single electrode model was constructed for a furnace. Current distribution was calculated by solving differential equation of magnetic field with AC input. In their model, Joule heating and thermal conduction were considered in heat transfer in solid charge and molten slag, and gas flow was not included. The temperature distributions in the solid charge and slag phase were predicted by solving the energy conservation equation. Temperature dependent electrical conductivities of charge, slag and electrode were considered. Thermal conductivity of charge included the effect of porosity and temperature. The heat generated by chemical reactions was evaluated with volumetric heat source or sinks above the slag/charge interface only. Furthermore, effect of various operating parameters such as electrode depth, electrical conductivity of the charge and the slag on power consumption was studied. In the same way as Sridhar and Lahiri [4], Ranganathan and Godiwalla [5] simulated the temperature distribution of the feed for a ferrochromium production furnace. Effects of bed porosity and charge preheating on the temperature distribution have been studied. The movement of the solid charge was assumed to be plug-flow, and the mean residence time to reach the slag surface was estimated to be about 12 hours. In their study, a 2-dimensional single electrode model was developed, and no flow behaviour for gas in the charge or molten slag and alloy was directly modelled.

Larsen et al. [6] developed a numerical 2-dimensional model for the AC arc in a 22 MW silicon metal submerged arc furnace, where the arc is the main energy source (~90%) in the silicon furnace, by using a CFD code FLUENT. Time dependent simulations have been carried out for a free-burning arc in a silicon metal furnace. The conservation equations for mass, momentum and energy together with time-dependent Maxwell's equations were solved. The model assumes symmetric furnace conditions, and takes one phase into consideration for a 3-phase submerged arc furnace. The AC arc model has not been integrated into a global gas flow simulation through the packed bed of the silicon furnace, which may include bulk gas flow, heat and mass transfer between the bulk gas and the feed materials.

Andresen and Tuset [7] modelled the fluid flow, heat transfer and heterogeneous chemical reactions above 1850°C in a similar 2-dimensional silicon sub-arc furnace of 8.7 MW, with a modified version of FLUENT. The AC arcs in the gas filled cavity were modelled with a DC arc. In their model, the furnace walls and electrode were treated as inert. The electric current and its effect outside the arc region are neglected. The metal pool was treated as a rigid body, thus no melt flow in the hearth. The active charge particles and the porous SiC bed were all treated with solid cylindrical vertical bars, but they can participate in the chemical reactions and change their height due to mass transfer. Also for silicon and ferrosilicon, Sævarsdottir et al. [8] reported a 2-dimensional Magneto Fluid Dynamics (MFD) model based on FLUENT to investigate the arc behaviour in the gas-filled cavities of the furnace, where the plasma arcs of SiO-CO based gas mixture are created. Both

laboratory and industrial arcs were simulated. However, the behaviour of the solid bed region and overall furnace thermal performance have not been included.

It could be seen that all the past research focused more on local transport phenomena of the submerged furnaces, such as the arc behaviour and the regions near the electrodes. All the studies were basically 2-dimensional models except by Sheng et al. [13-14] which are partially 3-dimensional for a SAF in nickel smelting. In this paper, various transport phenomena taking place in a typical submerged arc furnace will be analysed. A fully 3-dimensional CFD-based overall process model for ferrochrome production is proposed, and the potential and limits of the CFD model are addressed. All the relevant sub-models are individually described, including the flow in porous media for the packed bed, influence of electromagnetic body force on the flow, the electric and arc heating to the gas, solid charge and molten phase of slag and alloy, and the reduction kinetics which interact strongly with the heat transfer. The CFD-based process model for the submerged arc furnace, in principle, can handle fluid flow, heat and mass transfer for furnace gases, molten slag and alloy, and the solid feed. To show the principles and overall concept, a model for the gas flow in the solid packed bed is developed and described in this paper. More details are given on the development of a reaction kinetic model in relation to the CFD-based gas flow and heat transfer model, and future integration of the reaction kinetic model into process simulation are discussed.

2. PROCESS SIMULATION

Submerged arc furnaces for ferrochrome production are very complex in both physical and chemical aspects, and very difficult to control in practice. Generally speaking, the furnace can be divided into five regions: (1) gas region between the ceiling and the charge top, which is the off-gas consisting of about 90% CO; (2) packed bed region with solid and gas at upper part of the furnace with large temperature gradient, where the chromite ores are heated and reduced in solid state; (3) smelting region around electrode tips above the slag layer with a solid coke bed; (4) molten slag layer, where the oxides in the ore and flux form slag, and the unreduced chromite is dissolved into slag to be reduced further with the dissolved carbon from the alloy phase; and (5) molten alloy layer at bottom part of the furnace with relatively uniform temperatures. Energy required by the carbothermic reductions is supplied through the submerged arcs and electrical conduction in the solid bed and in the molten slag. The rate of solid state reduction is greatly affected by gas phase temperature distribution and gas flow pattern, as well as the structure of the feed. Figure 1 illustrates the complexity of the furnace interior and the smelting process for ferrochromium production, in comparison with Figure 2 for the dig-out of a ferromanganese production furnace [2].

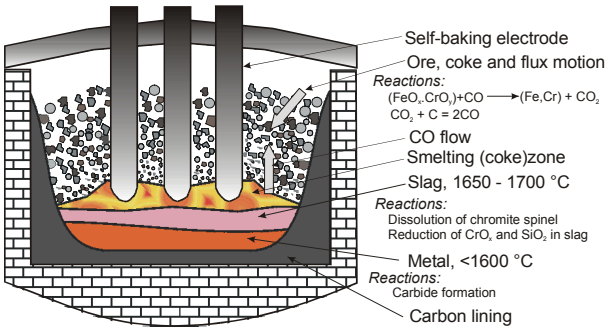

Figure 1. A schematic illustration of submerged arc furnace for chromite smelting.

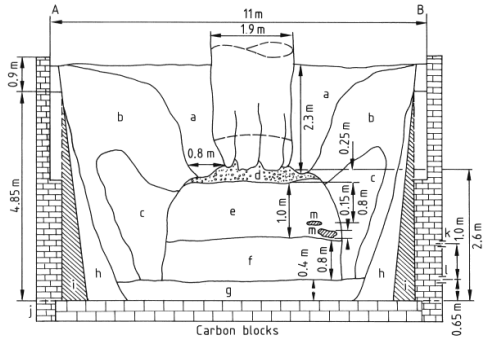

a) loosely sintered burden; b) loosely sintered material enriched in carbonaceous reducing agent; c)coke and slag region; d)coke bed; e) coke enriched layer; f) MnO melt layer with some slag, coke etc.; g)ferromanganese alloy layer mixed with MnO melt

Figure 2. Different zones of a FeMn submerged arc furnace [2].

In order to understand the transport process and to gain a better design and control of the furnace, a comprehensive process model is proposed for the submerged arc furnace. The inter-coupling of multi-physical and chemical phenomena in the system makes the simulation a very challenging task. Electric arc and conduction heating and their influence on the gas flow and the molten melt flow (both slag and alloy)

due to magneto-hydrodynamics (MHD) bring extra difficulties to the process simulation. The reaction kinetics of the gas - solid reduction process also play a critical role in the localised and overall energy and temperature distribution. Figure 3 gives an overview of the process model based on CFD framework, and the required sub-models.

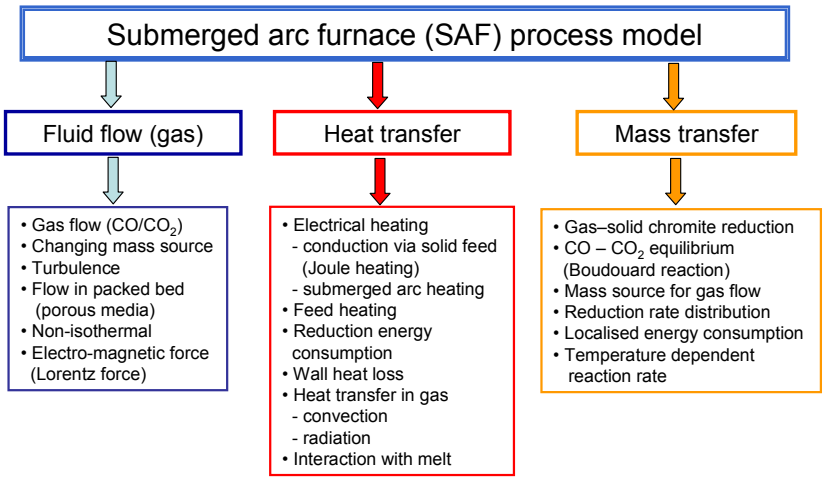

Figure 3. Overview of the CFD-based process simulation model for the submerged arc furnace process.

In order to construct an overall process model, the following three modules need to be considered, excluding the liquid phase phenomena. In principle, the transport process within the molten slag and alloy phase could also be added, but this will greatly increase the model complexity.

- Gas phase flow model within the solid packed bed.
- Heat transfer within the solid packed bed.
- Gas-solid reduction kinetics, which provides variable heat sinks to heat transfer and mass source for flow.

Below is a detailed description of the transport phenomena and required sub-models, as well as their interactions.

2.1 Gas flow within the packed bed

Gases are generated in the furnace beneath and nearby the electrodes from the reduction reactions of the chromite pellet (or lumpy ores) with CO in the packed bed and from the smelting reduction of the dissolved chromium oxides with carbon in the slag. The precise treatment of the flow in the packed bed in this case is difficult, because the CO is not only coming into the flow field through a fixed boundary like the slag surface – it is continuously produced within the packed bed, especially at high temperature zones. The following global reduction reactions may explain the mass source, which are the flow media in the packed bed.

a) Solid-state: Chromite reduction in the packed bed and Boudouard reaction:

$$FeCr_2O_4 + 4CO_{(g)} \rightarrow 2Cr + Fe + 4CO_{2(g)} \quad \text{(Solid-state reduction with CO)} \quad (1)$$

$$CO_{2(g)} + C \rightarrow 2CO_{(g)} \quad \text{(The Boudouard reaction)} \quad (2)$$

$$FeCr_2O_4 + 4C \rightarrow 2Cr + Fe + 4CO_{(g)} \quad \text{(Overall reaction)} \quad (3)$$

b) In molten slag: Chromite reduction at slag-metal interface by dissolved carbon in the alloy phase, releasing CO on the slag surface to the packed bed:

$$(FeCr_2O_4) + 4[C] \rightarrow 2[Cr] + [Fe] + 4CO_{(g)} \quad (4)$$

The Boudouard reaction is the source of CO reducing gas. In the presence of coke particles throughout the packed bed, the CO gas dominates the gas-phase composition (90% of the off-gas composition). In order to properly model the gas flow, the mass source coupled with solid state reduction of chromite and the Boudouard reaction have to be taken into account. CO generation rate ($\dot{m}_{CO}$, kg/s·m^3) as a function of temperature (T, °C), time (t, minute) has to be developed based on reduction rate equation obtained from experiments, i.e. $\dot{m}_{CO} = f(T,t)$.

The second important feature of the gas flow in the packed bed is that it is highly non-isothermal, and affected by the Lorentz force due to varying electromagnetic field. Since the main energy source comes from the electrodes via arcs and electrical conduction, a large temperature gradient is introduced from near the electrode tips above the slag layer to the surface of the packed bed. This has to be linked to the energy supply and consumption mechanisms: electrical heating by arcs and conduction, and energy consumption due to chromite reduction.

2.2 Heat transfer within the solid packed bed

Heat transfer and temperature distribution within the packed bed are key aspects of the production process. Therefore both energy consumption (heat sink) due to chromite reduction and energy supply (heat source) due to electrical heating have to be defined. It is known that the reduction rate is highly dependent on temperature, and the chromite reduction is a highly energy consuming process. To define the reaction heat sink, the reaction energy consumption as a function of local reduction rate needs to be supplied based on the reaction kinetic model. This can be further obtained from the reduction degree equation and reaction enthalpy of the overall reaction. Electrical conduction, the Joule heating, partly determines the energy dissipation, while the arc heating by hot ionised gases contributes greatly to the energy dissipation in the packed bed. Therefore, definition of the heat source in the system becomes as important as the definition of the heat sinks due to chromite reduction. In order to precisely characterise the system, the electrical field (current and potential) and arc behaviour have to be resolved, which for the complete furnace model is a challenging task.

As an alternative, simple volumetric heat source and sinks could be utilised to represent the heat source and sinks. This has been used in the initial stage for the construction of the overall process model. The developed models for reaction rate, mass source and energy sink will be introduced into the CFD process model in the future. Electrical conduction and arc heating model will be developed after the coupling mass source and energy sink due to chromite reduction.

2.3 Gas – solid reduction kinetics

As is indicated in 2.1 and 2.2, chromite reduction kinetics are the key for the gas phase flow and heat transfer within the packed bed. The focus of this research has been placed on the gas-solid reduction kinetics and preparation of the kinetic data in a form which is suitable and convenient for the flow and heat transfer calculation in the overall process model. There are essentially two aims in the reduction kinetic model: (1) development of a temperature dependent model for supplying the mass source for gas flow and reduction degree for the packed bed, and (2) development of an energy model for supplying energy consumption or heat sinks, depending on reduction degree and temperature.

2.4 Flow and heat transfer in the molten phase

Although the slag and alloy phases are very important aspects of the chromite smelting, a model including gas and solid packed bed as well as molten melts of slag and alloy is too ambitious to accomplish at this stage. Thus, the transport phenomena such as flow (free surface and electromagnetic stirring), heat transfer (natural and forced convection, and Joule heating) and further reduction reactions (smelting reduction) within the molten phase are not included in this study. The slag – gas interface is treated with a fixed mass source and thermal boundaries. The focus is put on the gas – solid interactions in the upper part of the furnace.

It is obvious that to simulate all the aspects of the chromite smelting in one model is very difficult (if not impossible) due to the coupled transport processes in such a complex furnace. Therefore only certain aspects could be simulated with reasonable assumptions, and priority has to be given to modelling the most important phenomena in the process. In this way, the process model can be developed step by step to increase process complexity.

3. SOLID STATE REACTION KINETICS

The reduction of chromite pellet takes place mainly in the solid state by the generated CO gas in the lower part of the furnace, in the slow descending packed solid bed. In addition, partial smelting reduction also occur in the molten slag phase, where the coke particles react with dissolved chromium oxides and generate CO gas (which evolves out of the slag layer and enters into the solid bed as reductant) and metallic Cr (which reports to alloy phase). The majority of the CO as reactant in the packed bed comes from the Boudouard reaction when CO_2 is in contact with coke particles. It is assumed that the direct reduction of the chromite ore/pellet by carbon particles is negligible in the packed bed. The chromite is mainly reduced with CO gas, which is constantly supplied via Boudouard reaction. The reduction of chromite pellet with CO gas is characterised by different interrelated mechanisms and steps. Due to the presence of iron oxides together with chromium, step-wise reduction of iron oxides must also be considered. In the development of the kinetic relationship, only the global reduction reaction is utilised.

Two of the major charges in SAF for reduction with CO, sintered pellets and lumpy ore, were studied experimentally [15-17] and modelled mathematically with a grain model [18]. In order to obtain the CO mass source and heat sink due to chromite reduction, high temperature experiments on chromite pellet reduction were conducted to determine reduction rate at various conditions. The reduction degree X has been determined at various temperatures as a function of time, where X is defined as the removed oxygen over total reducible oxygen in the chromite pellet. Reduction degree X together with the Boudouard reaction can be linked to the CO generation rate, which can be used to supply energy sinks to the heat transfer model.

$$X = \frac{\text{Removed oxygen by CO}}{\text{Total reducible oxygen in the chromite}} \times 100\% \tag{5}$$

The calculated reduction degree as function of time based on the experimental data under various conditions is shown in Figure 4. It is seen that both sintered and lab-prepared pellets have higher reduction rates than the lumpy ore. Higher temperature and especially the presence of coke particles around the ore will promote the reduction rate. Faster and more complete reduction was reported by Vazarlis and Lekatou [19] with chromite particles mixed with coke, not pellets, and almost 100% reduction was reached within 60 min at 1500°C. Figure 5 shows chromite reduction at elevated temperatures, at a constant heating rate of 10°C/min by Vuuren [20] and 2.5°C/min by Kekkonen et al. [16]. In considering the mean residence time of the pellets and the temperature gradients from the top to the bottom of the packed bed, the mean heating rate would be around 2°C/min. Therefore, the reduction curve at 2.5°C/min heating curve may represent approximately the furnace conditions, and a correlation was made between the reduction degree and temperature at this constant heating rate, as follows:

$$X = 7.40\times10^{-3}(T-700) - 2.5\times10^{-6}(T-700)^2 + 6.83\times10^{-6}(T-700)^3 \ \text{(T, °C)} \tag{6}$$

$$\text{or} \qquad X = 1.85\times10^{-2}t - 1.56\times10^{-5}t^2 + 1.07\times10^{-4}t^3 \ \text{(t, min)} \tag{7}$$

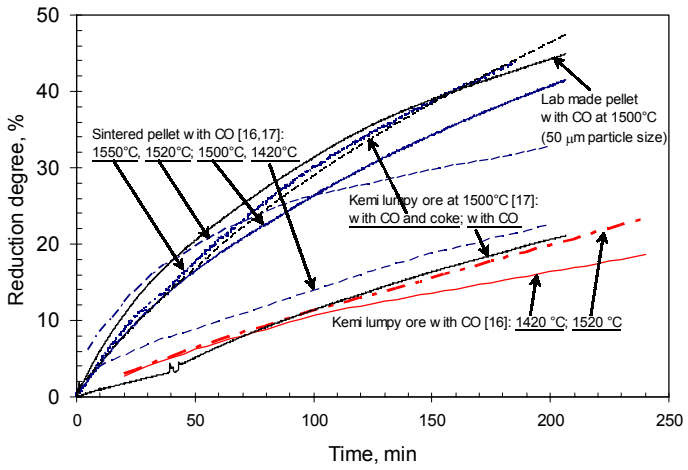

Figure 4. Comparison of chromite reduction under different conditions.

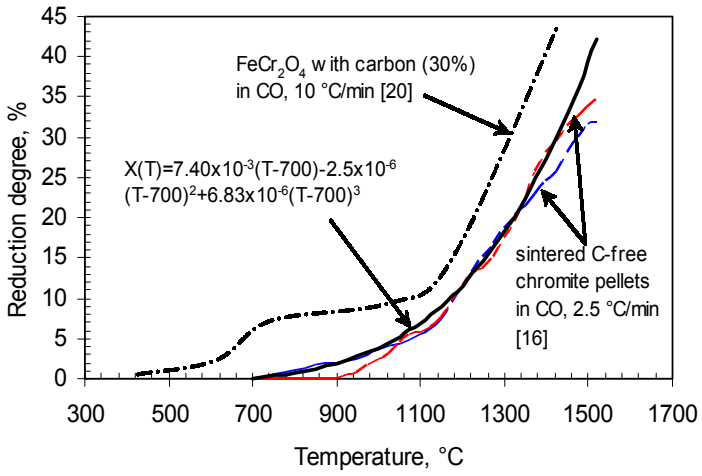

Figure 5. Reduction degree of chromite as a function of temperature.

In order to supply the energy sink due to chromite reduction, reduction enthalpy at different temperatures was calculated with HSC Chemistry [21], based on individual reduction reactions of chromium and iron containing oxides. The results are illustrated in Figure 6. The CO regeneration due to the Boudouard reaction was included. At high temperatures, the Boudouard reaction is fast, and thermodynamic equilibrium can be assumed. Figure 7 shows the average reaction enthalpy as a function of reduction degree in the temperature range of 400 to 1600°C. The reduction reactions include Cr_2FeO_4, Fe_3O_4, FeO, Cr_2O_3 and $MgCr_2O_3$. The overall reaction heat was established based on the thermodynamic reducibility of the reducible oxides (step-wise selective reduction), chromite compositions, and the individual reaction heat. The experimental results showed gradual composition changes in the Fe/Cr ratio, from the analysis of the metal droplets, across the pellet. It is obvious that when iron oxide reduction has proceeded far enough, chromium oxide starts to be reduced and the metallic chromium formed dissolves in any available Fe-based metal phase. Figure 8 shows the reaction enthalpy as a function of temperature and the curve-fitted formula. Since the temperature effect is small, a generalised reaction enthalpy as function of reduction degree can be represented as follows:

$$\Delta H = 166 + 386X + 124X^2 - 108.5X^3 + 685.5X^4 \ \ (kJ / mole\,C\,consumed) \tag{8}$$

or $$\Delta H = 252 - 4.66\times10^{-3}T - 1\times10^{-6}T^2 (kJ / mole\,C\,consumed) \tag{9}$$

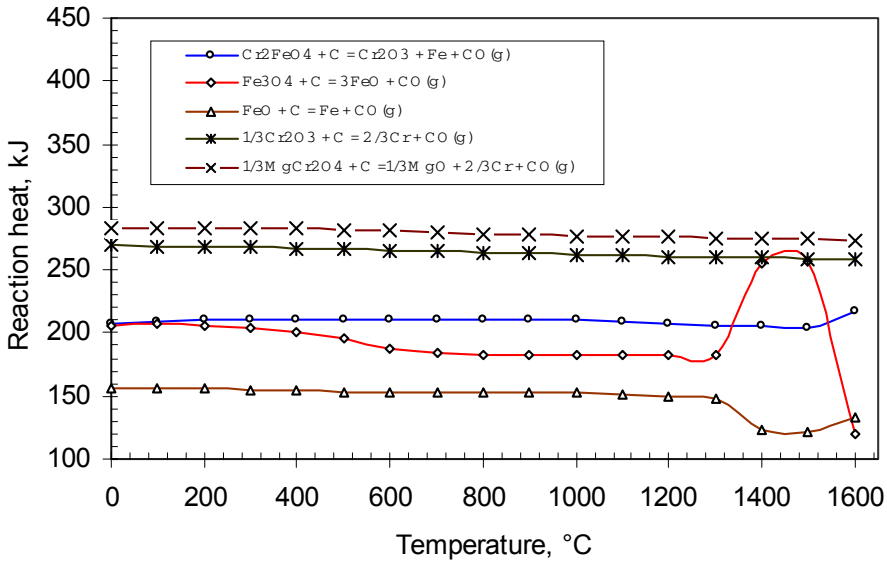

Figure 6. Reaction heat (kJ/mole C) for the reduction of the main reducible constituents.

In addition to the experimental results and the empirical correlations of reduction degree and temperature, it is essential to establish a mathematical reaction model, which can approximately describe the chemical reactions within the furnace charge, and further be integrated with the process modelling. Therefore, a modified grain model has been developed [18], in which it is assumed that a spherical pellet of the solid reactant consists of a large number of spherical chromite grains of uniform size.

The pellet sample is in contact with a reacting gas (CO) to form a solid product and a gaseous product (CO_2). It is expected that the model will be integrated into the CFD-based process model in the near future.

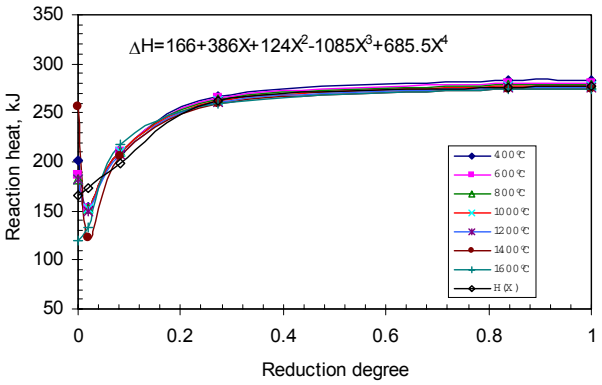

Figure 7. Reduction heat (kJ/mole C) as a function of reduction degree.

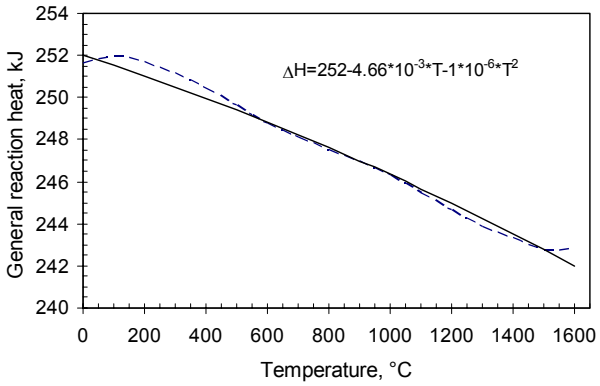

Figure 8. Reduction heat (kJ/mole C) as a function of reduction temperature (°C).

4. COMPUTATIONAL FLUID DYNAMICS (CFD) MODEL

Computational fluid-dynamics (CFD) is a very useful tool in process simulation of transport phenomena of industrial processes. In CFD, the governing partial differential equations are numerically solved for the conservation of mass, momentum, heat and chemical species in fluid-flow systems. CFD modelling generates detailed distributions of velocity, temperature, concentration of species, and other flow-related variables in all dimensions of the reactors and furnaces. CFD has nowadays become an integral part of the engineering design and analysis environment in the process industry because of its ability to predict the performance of new designs or processes before they are ever manufactured or implemented. Many general purpose commercial packages have been available on the market for over two decades. Considering the functionality and limitations of general purpose CFD code, specific attention is required in the SAF model to couple the Maxwell's equations and reaction kinetic model to the solver. At the first stage, to illustrate the overall process model, a simplified CFD model was built with a general CFD code for an industrial scale SAF for ferrochrome production. The gas flow and heat transfer within a submerged arc furnace for high carbon ferrochrome production were simulated.

Table 1. Furnace dimensions and major operating conditions for the current process model.

Item	Details	Remarks
Production data:		
Alloy production rate	120 t/day (5t/hour)	Alloy composition:
Slag temperature (°C)	1700	70%Cr-1.5%Si-5%C + rest Fe
Off-gas generation rate (Nm^3/h)	3000 (100% CO)	From slag phase and electrode tips
Coke consumption (kg/t alloy)	400	
Energy consumption (kWh/t alloy)	4000	
Furnace dimensions		
Hearth diameter (mm)	8385	Similar to the furnace in reference [5].
Electrode diameter (mm)	1350	
Pitch circle diameter (mm)	3290	
Height of the solid charge (mm)	3190	
Distance from the electrode tip to the slag layer (mm)	1100	

4.1 Furnace description

To construct a CFD model, detailed process data are required. Therefore, a real industrial furnace for high carbon ferrochromium (70% Cr and 5% C) production was used as the main reference to deduce and define the furnace dimensions, productivity, and boundary conditions. Based on the basic information in the literature [5], furnace production of 120 t/day was estimated. The estimated effective power of the furnace is 20 MW, based on an average energy consumption of 4000 kWh/t alloy. The mean residence time of the feed within the furnace was estimated as 12 hours [5]. The feed smelting capacity is estimated roughly as 400 t/day. The basic furnace dimensions are listed in Table 1.

4.2 CFD model and preliminary results

A general purpose CFD code Phoenics 3.4 [22] was used to generate the basic furnace model. The model is fully 3-dimensional, including 3 electrodes, a solid feed packed bed, a coke bed beneath the electrode tips, and an open space between the ceiling and solid feed. In the current model, only gas phase behaviour was simulated. Solid feed and coke particles only provide resistance to gas flow, and reaction energy consumption was estimated as a volumetric heat sink in different zones of the furnace. The slag and alloy layer provide part of the CO source for the packed bed.

Electrical and arc heating were taken as volumetric heat sources. It was also assumed that energy consumption due to chromite reduction takes places partly in the solid state and partly in the slag phase. The influence of electromagnetic field on gas flow is neglected. Gas mass flow (CO) was assumed to originate partially from the slag phase at 1700°C and partially from the three electrode tips at 2500°C. To get effective energy dispersion (arcs and Joule heating), a higher thermal conductivity gas was used to simulate the electrical heating, before the real arcs and Joule heating were modelled. For the furnace geometry, only the interior was considered, and the inner walls of the furnace were assumed adiabatic since the total heat loss is small in comparison with the overall energy supply and consumption by the reduction reactions.

CO gas flow originating from the slag surface and the three electrode tips was modelled with the standard k-ε turbulence model, and the flow resistance was coded with Ergun's equation by assuming a constant bed porosity of 0.2 in the solid feed region and coke zone. In the future, variable porosity within the bed will be explored, due to the size distribution and shape of feed charge (coke particles and pellets, and/or lumpy ores). A gas phase radiation model Immersol (Immersed solid) from Phoenics was used to simulate radiative heat transfer. The influence of the solid particles in the packed bed on the thermal radiation will be studied further in the future. Figure 9 and Figure 10 show the predicted temperature distribution at various cross sections of the furnace. The maximal gas temperature could be as high as 2300°C below the electrode tips in the arc zone, and near the furnace roof a temperature about 600°C is predicted. Clearly, a large temperature gradient in the packed bed is observed. Figure 11 shows the predicted gas velocities beneath the electrodes and near the furnace roof. At the upper part of the furnace, the gas flows around the electrodes and bends toward the off-gas duct. Figure 12 illustrate the calculated pressure distributions of the gas phase beneath the electrodes and across two of the three electrodes. The pressure drop through the packed bed was estimated to be over 200 Pa.

The thermal behaviour in SAF is dominated on one hand by the electrical energy supply and bed properties as energy source, and on the other by the reduction kinetics as energy sinks. As the next step, the energy consumed by the chromite reduction will be coupled into the CFD model as a function of temperature and location, and supplied to the energy equation in the CFD code. In this way, a more reasonable temperature distribution and reduction rate will be achieved when the energy supply and flow field are solved with simultaneous solution of Maxwell's equations. The localised mass generation of CO from the reaction kinetics will also be linked to mass conservation and eventually momentum transport. Furthermore, the flow and heat transfer in the slag and/or molten alloy phase can also be included, as part of our future plan to gradually add more aspects as mentioned above to the overall process model.

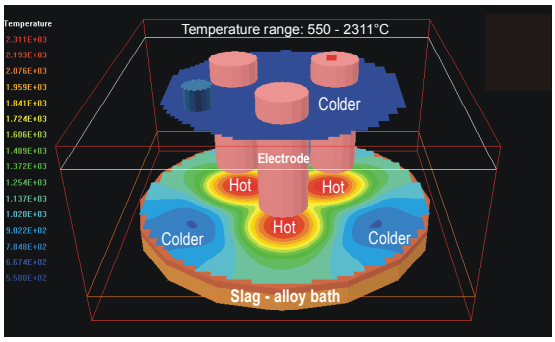

Figure 9. Predicted temperature distribution below the electrodes and near the roof.

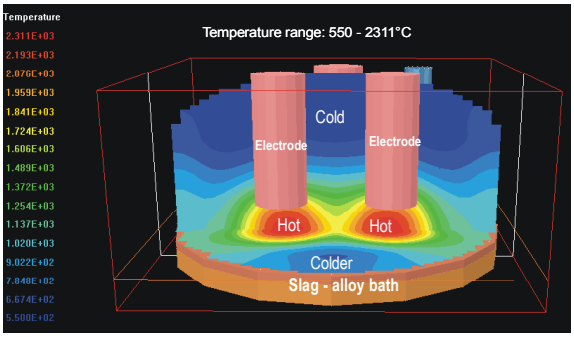

Figure 10. Predicted temperature distribution across electrodes and above slag layer.

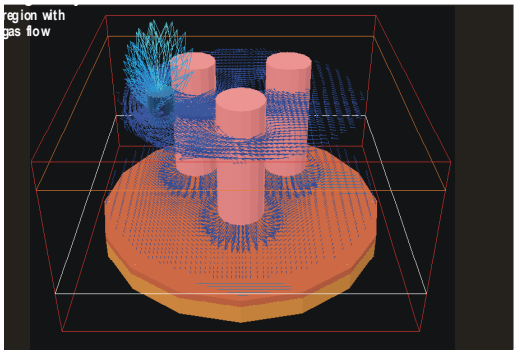

Figure 11. Predicted velocity vectors beneath electrodes and below the roof.

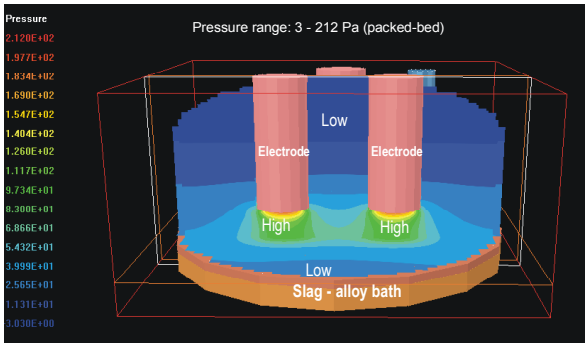

Figure 12. Predicted pressure distribution across electrodes and above slag layer.

5. SUMMARY

In the present paper, an overall process simulation model is presented for a submerged arc furnace in ferrochromium production. For optimised operation of the process, there is a great need for such a comprehensive model, which can simulate the fluid flow, heat transfer and reduction kinetics. Various transport phenomena within the submerged arc furnace are described which include fluid flow, electrical and arc heating, electromagnetic body forces, and reaction kinetics, as well as their interactions. Solid state reduction kinetic data were prepared based on high temperature experiments and curve-fitted correlations are presented to provide the mass source for the gas flow, and energy sink for heat transfer. To illustrate the concept, a fully 3-dimensional CFD model for a 120 t FeCr alloy/day SAF furnace was presented under simplified conditions. In this model, the heat source due to electrical and arc heating and heat sink due to chromite reduction were simplified as volumetric heat sources and heat sinks, so as to generate a reasonable temperature distribution within the packed bed region of the furnace. The CO was assumed to originate from the electrode tips and the slag phase reduction. In the model, only gas phase behaviour was simulated, however, the solid phase provides friction to the gas flow and cause pressure drop. The pressure drop was modelled with Ergun's equation by assuming a fixed bed porosity and average particle size of the pellets and coke.

It should be emphasised that the present CFD model only illustrates the structure, complexity and capability of the overall process model, and the possibly expected results. At the moment, a lot of model development work is under way to tackle each individual sub-model. In the next step, localised mass sources for CO and energy sinks for heat transfer will be coupled to the CFD model. Then the electrical and arc heating will be included by solving Maxwell equations to provide electrical potential and current fields. It is expected that the future model will predict more accurately the temperature distribution of the gas, distribution of the reduction degree or metallization of the feed, influence of various operating conditions such as feed porosity change, electrode penetration depth, power level, and influence of furnace geometry variations. The simulation results after validation will greatly help process modification and re-design of such furnaces, and eventually lead to a better furnace control.

6. REFERENCES

[1] Wedephol A. and Barcza N.A., "The 'dig-out'of a ferrochromium furnace". *Spe. Publ. Geol. Soc. S. Afr.,* 7, 1983. pp. 351-363.

[2] Kousaris A. and See J.B., "Reactions in the production of high carbon ferromanganese from Mamatwan ores". *J. S. Afri. Inst. Min. Metall.*, 19, 1979, pp. 149-158.

[3] Reuter M.A. and Yang Y., "40.4 Metallurgical Process Control", *Smithells Metals Reference Book*, 8th edition, ed. W.F. Gale, Butterworth-Heinemann. In press.

[4] Sridhar E. and Lahiri A.K., "Steady state model for current and temperature distributions in an electric smelting furnace". *Steel Research*, 65(10), 1994, pp. 433-437.

[5] Ranganathan, S. and Godiwalla, K.M., "Effect of preheat, bed porosity, and charge control on thermal response of submerged arc furnace producing ferrochromium". *Ironmaking and Steelmaking (UK),* 28(3), 2001, pp. 273-278.

[6] Larsen H.L., Gu L. and Bakken J.A, "A numerical model for the AC arc in the silicon metal furnace". *INFACON 7*, Eds. Tuset J.Kr., Tveit H. and Page I.G., FFF, Trondheim, Norway, June 1995, pp.517-527.

[7] Andresen B. and Tuset J.K., "Dynamic model for the high-temperature part of the carbothermic silicon metal process". *INFACON 7*, Eds. Tuset J.Kr., Tveit H. and Page I.G., FFF, Trondheim, Norway, June 1995, pp.535-544.

[8] Sævarsdottir, G.A., Bakken, J.A., Sevastyanenko, V.G. and Gu, L., "Modelling of AC arcs in submerged-arc furnaces for production of silicon and ferrosilicon". *Iron and Steelmaker (USA),* 28(10), 2001, pp.51-57.

[9] Szekely J., McKelliget J. and Choudhary M., "Heat transfer, fluid flow and bath circulation in electric-arc furnaces and DC plasma furnaces", *Ironmaking and Steelmaking*, 10(4), 1983, pp. 169-179.

[10] Caffery G., Warnica D., Molloy N. and Lee M., "Temperature homogenisation in an electric arc furnace steelmaking bath", *Proceedings of the International Conference on CFD in Mineral and Metal Processing and Power Generation*, CSIRO 1997. pp. 87-99.

[11] Gunnewiek L.H. and Tullis S., "Prediction of heat and fluid flow in the slag phase of an electric arc reduction furnace", *Proceedings of the International Symposium on Computational Fluid Dynamics and Heat/Mass Transfer Modelling in the Metallurgical Industry*, eds. S.A. Argyropoulos and F. Mucciardi, August 24 - 29, 1996, Montreal, Quebec. CIM. pp.250-264.

[12] Hasegawa N. and Kaneda A, "Optimization of continuous slag/matte separation in Mitsubishi process by using numerical heat and fluid flow analysis". *Materials Processing in the Computer Age III*, eds. V.R. Voller and H. Heinen, in 2000 TMS Annual Meeting in Nashville, Tennessee, March 12-16, 2000. TMS Warrendale. pp.51-60.

[13] Sheng Y.Y., Irons G.A. and Tisdale D.G., "Transport phenomena in electric smelting of nickel matte: Part I. Electrical potential distribution". *Metall. and Mat. Trans. B*, 29B(1), 1998, pp. 77-83.

[14] Sheng Y.Y., Irons G.A. and Tisdale D.G., "Transport phenomena in electric smelting of nickel matte: Part II. Mathematical modelling". *Metall. and Mat. Trans. B*, 29B(1), 1998, pp. 85-94.

[15] Kekkonen M., Xiao Y. and Holappa L., "Kinetic study on solid state reduction of chromite pellets". *INFACON 7*, 1995, Trondheim, pp.351-360.

[16] Kekkonen M., Syynimaa A., Holappa L. and Niemela P., "Kinetic study on solid state reduction of chromite pellets and lumpy ores". *8th International Ferroalloys Congress Proceedings: INFACON 8*, CSM, Beijing, China, June 1998, pp.141-146.

[17] Xiao Y., Schuffeneger, C., Reuter M., Holappa L. and Seppälä T., "Solid state reduction of chromite with CO". Accepted for publication in: *INFACON 10*, Cape Town, S. Africa, 2004.

[18] Xiao Y., Reuter M.A. and Holappa L., "Kinetic modelling of chromite pellet reduction with CO gas under rising temperatures from 700 to 1520°C". *Proceedings of the Ninth International Ferroalloys Congress and the Manganese 2001 Health Issues Symposium: INFACON 9.* Ferroalloy Association, Quebec City, Canada, June 2001. pp.

[19] Vazarlis H.G. and Lekato, A., "Pelletising-sintering, prereduction, and smelting of Greek chromite ores and concentrates". *Ironmaking and Steelmaking*, 20 (1), 1993, pp.42-52.

[20] Vuuren,C.P.J. Van Bodenstein J.J., Sciarone M. and Kesten, P., "The reduction of synthetic iron chromite in the presence of various metal oxides – a thermo-analytical study". *Proceedings of the 6th International Ferroalloys Congress*: *INFACON 6, Volume 1*. Cape Town, S. Africa, 1992, SAIMM, Johannesburg, pp.51-55.

[21] Roine A., *HSC Chemistry® 5.0*. Outokumpu, 2002.

[22] Cham, *Phoenics: Parabolic Hyperbolic Or Elliptic Numerical Integration Code Series*, http://www.cham.co.uk. (accessed in December. 2002)